

Structure of the magnetotail current: Kinetic simulation and comparison with satellite observations

Paolo Ricci,^{1,2} Giovanni Lapenta,^{1,3} and J. U. Brackbill³

Received 2 December 2003; revised 4 February 2004; accepted 13 February 2004; published 16 March 2004.

[1] The results of a three-dimensional kinetic simulation of a Harris current sheet are used to show and reproduce the ISEE-1/2, Geotail, and Cluster observations of the magnetotail current sheet structure. Current sheet flapping, current density bifurcation, and reconnection are explained as the results of the evolution of a Harris current sheet, where lower-hybrid drift, kink, and tearing instabilities are involved. **INDEX TERMS:** 2744 Magnetospheric Physics: Magnetotail; 2753 Magnetospheric Physics: Numerical modeling; 2764 Magnetospheric Physics: Plasma sheet; 7843 Space Plasma Physics: Numerical simulation studies; 7835 Space Plasma Physics: Magnetic reconnection. **Citation:** Ricci, P., G. Lapenta, and J. U. Brackbill (2004), Structure of the magnetotail current: Kinetic simulation and comparison with satellite observations, *Geophys. Res. Lett.*, 31, L06801, doi:10.1029/2003GL019207.

1. Introduction

[2] At the end of April 2, 1978, the ISEE-1/2 spacecraft detected a flapping of the plasma sheet, crossing the central region more than 10 times in an hour [Sergeev *et al.*, 1993]. More recently, time analysis of data from the four Cluster spacecrafts [Balogh *et al.*, 2001] shows that the current sheet dynamics are characterized by a wave-like transient that propagates in the dawn-to-dusk direction [Sergeev *et al.*, 2003; Runov *et al.*, 2003], which is interpreted as the signature of a kink or sausage instability [Runov *et al.*, 2003]. Karimabadi *et al.* [2003a, 2003b] argue that the ion-ion kink instability causes a displacement of the current sheet that explains the flapping observations.

[3] During a “turbulent” crossing, ISEE-1/2 detected current concentrations outside the central region, unlike the Harris current sheet [Sergeev *et al.*, 1993]. Geotail averaged data obtained from October 1993 to June 1995 [Kokubun *et al.*, 1994; Mukai *et al.*, 1994] show that the structure of the plasma sheet often can be approximated by a double-peaked electric current sheet [Hoshino *et al.*, 1996] and observations made by the same spacecraft during a substorm on 23 April 1996 lead to a similar conclusion [Asano *et al.*, 2003]. On January 14, 1994, Geotail also detected multiple double-peaked current sheet crossings, associated with plasma flow [Hoshino *et al.*, 1996]. More recently, time analysis of data from the four Cluster space-

crafts [Balogh *et al.*, 2001] showed that fast motion and bifurcation of the current sheet are associated with a wave-like transient propagating in the dawn-to-dusk direction [Sergeev *et al.*, 2003; Runov *et al.*, 2003]. Generalizations of the standard Harris current sheet equilibrium recently have been proposed to reproduce the bifurcation observed by satellites [Shindler and Birn, 2002; Sitnov *et al.*, 2003]. Zelenyi *et al.* [2002] show that non-adiabatic effects can reduce the current density in the center of the current sheet. Arzner and Sholer [2001] remark that a bifurcated current sheet can be present in the plasma outflow region when magnetic reconnection is occurring. Karimabadi *et al.*, [2003a, 2003b] interpret the bifurcated structure of the current sheet as the evolution of the magnetic field profile due to the kink instability.

[4] Plasma flow has also been observed during a substorm event [Hoshino *et al.*, 1996; Øieroset *et al.*, 2001; Asano *et al.*, 2003]. Generally, plasma flow is explained in terms of plasma out-flowing from a reconnection region.

[5] We remark that the observations refer both to the distant magnetotail ($\approx 100 R_E$) [Hoshino *et al.*, 1996] and to a region closer to Earth ($\approx 15 R_E$) [Sergeev *et al.*, 1993; Asano *et al.*, 2003; Runov *et al.*, 2003; Sergeev *et al.*, 2003].

[6] The present work analyzes the results of a three-dimensional kinetic simulation of the Harris current sheet by introducing diagnostic tools very similar to those used by satellites. We show that the evolution of a Harris current sheet can be responsible for the data observed by the satellites described in the references above. We recover the most significant magnetic data records obtained as a signature of current sheet flapping. The occurrence frequency of the magnetic field B_x allows a comparison with observations by GEOTAIL [Hoshino *et al.*, 1996] that show current bifurcation, and signatures of bifurcation observed in single crossing are also recovered. We also analyze the plasma flow due to the tearing instability.

2. The Simulations

[7] In our study, we use the implicit PIC code CELESTE3D [Brackbill and Forslund, 1985], which is particularly suitable for large scale and long period kinetic simulations performed with high mass ratios. We use the same plasma parameters as the GEM challenge [Birn *et al.*, 2001]. We start from a standard Harris current sheet. The magnetic field is given by $B_x(z) = B_0 \tanh(z/\lambda)$, and density by $n(z) = n_0 \cosh^{-2}(z/\lambda) + n_b$, with $\lambda = 0.5 c/\omega_{pi}$, $T_i/T_e = 5$, the ion drift velocity $V_{i0} = 1.67 V_A$, and a background population with density $n_b = 0.2 n_0$. We define the Alfvén speed, V_A , the plasma frequency, ω_{pi} , the ion cyclotron frequency, ω_{ci} , and the ion Larmor radius, ρ_i , using n_0 and B_0 . Unlike the GEM challenge, we do not add any initial

¹Istituto Nazionale per la Fisica della Materia (INFN), Dipartimento di Fisica, Politecnico di Torino, Torino, Italy.

²Dipartimento di Energetica, Politecnico di Torino, Torino, Italy.

³Theoretical Division, Los Alamos National Laboratory, Los Alamos, New Mexico, USA.

perturbation and let the system evolve on its own. The dimensions of the system are $[-L_x/2, L_x/2] \times [-L_y/2, L_y/2] \times [-L_z/2, L_z/2]$ with $L_x = 12.8 c/\omega_{pi}$, $L_y = 19.2 c/\omega_{pi}$, and $L_z = 6.4 c/\omega_{pi}$. Our grid has $N_x \times N_y \times N_z = 32 \times 48 \times 32$ cells. The boundary conditions assume perfect conductors at $z = \pm L_z$ and periodic boundaries in x and y . The mass ratio is $m_i/m_e = 180$. The parameters we have chosen make the current sheet particularly unstable so that its dynamics are accelerated compared with typical magnetotail current sheets, and thus can be modelled in a reasonable computational time. As a consequence, it is necessary to scale our results to make a quantitative comparison between simulation results and observations.

[8] The simulation shows the development of the fastest Lower-Hybrid Drift Instability (LHDI) on the electron gyroscale, followed by electromagnetic modes with wavelengths intermediate between the ion and the electron gyroscale. The background population, which contributes a velocity shear to the initial conditions, triggers a Kelvin-Helmholtz (KH) or ion-ion kink instability [Karimabadi *et al.*, 2003a, 2003b]. A tearing instability also develops that leads to plasma inflow and out-flow jetting.

3. Current Sheet Flapping

[9] Clear evidence of current sheet flapping is shown by ISEE-1/2 [Sergeev *et al.*, 1993], by Geotail [Hoshino *et al.*, 1996], and by Cluster [Runov *et al.*, 2003; Sergeev *et al.*, 2003]. We show that the current sheet kinking that develops in the course of our simulations can explain Cluster observations.

[10] Figure 1 shows fully developed current sheet kinking. The B_x field is shown. The wavelength is $k_y \lambda \approx 0.5$, which matches fairly well the observed wavelength by Runov *et al.* [2003] ($k_y \lambda = 0.7$). The linear theory predicts a decrease of the wavelength when ρ_i/λ increases [Karimabadi *et al.*, 2003a], consistent with the fact that our thickness is likely smaller than the observation. The amplitude $A/\lambda \approx 2$ at time $t\omega_{ci} = 16$ is comparable to the observed value ($A/\lambda \approx 1.4$) [Sergeev *et al.*, 2003]. The flapping motion observed by Cluster is moving duskward at $v_{ph} \approx 200$ km/s, corresponding to approximately $0.2 V_A$. The kink instability shown in our simulations gives a $v_{ph,SIM} \approx 0.5 V_A$, larger than observed in space. However, the linear theory predicts a decrease of the phase velocity when ρ_i/λ increases. Thus our use of an artificially high ρ_i/λ explains our higher phase speed and is consistent with our interpretation of the flapping motion.

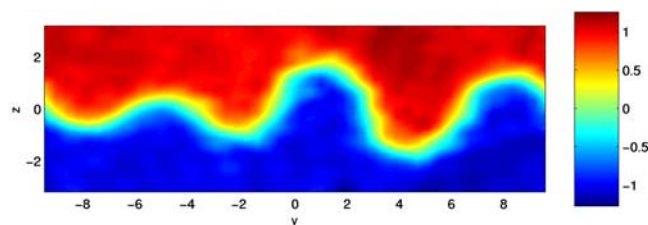


Figure 1. The kink of the current sheet is presented by showing the x component of magnetic field, B_x as a function of y and z , at time $t\omega_{ci} = 16$ and at $x = 0$. B_x is normalized to B_0 .

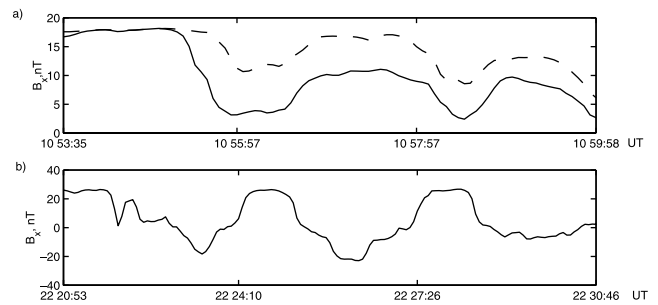


Figure 2. Signatures of current sheet flapping, observed by the FGM Cluster experiment [Balogh *et al.*, 2003]. We report the B_x magnetic field recorded by satellites #2 (dashed) and #3 (solid) on 29 August 2001 that has been described by Runov *et al.* [2003] (a), and by satellite #3 on September 26, 2001, described by Sergeev *et al.* [2003] (b).

[11] In Figure 2a we show Cluster #2 and #3 observations taken on 29 August 2001, which have been analyzed previously by Runov *et al.* [2003]. In Figure 3a, we evaluate the magnetic field as a function of time as would be recorded by a virtual spacecraft placed in the environment provided by the simulation. Consistent with the real spacecraft disposition, we impose a separation between the two virtual satellites in the z direction of the order of $\lambda/2$. Cluster observes an oscillation period of $\tau = 90$ s and a relative velocity between satellite and plasma $v_{ph} \approx 0.2 V_A$. In order to decrease the time necessary for the observation, we increase the relative satellite velocity to $v_{SIM} = 5 V_A$, which decreases the oscillation period to $\tau_{SIM} = 2 \omega_{ci}^{-1}$. This is in good agreement with the oscillation period recorded by Cluster, provided that the oscillation period is rescaled to the relative velocity between the satellite and the plasma. In fact, as $\omega_{ci} \approx 0.6 s^{-1}$ in the magnetotail, the observed wavelength, $v_{ph}\tau \approx 11 c/\omega_{pi}$, and the simulated wavelength, $v_{SIM}\tau_{SIM} \approx 10 c/\omega_{pi}$, are comparable. The magnetic data refer to a period between $t\omega_{ci} = 11$ and $t\omega_{ci} = 14.5$ when the kink instability has already developed, but its amplitude still allows satellite trajectories that do not cross the current sheet.

[12] The flapping observed by Cluster #3 on September 26, 2001 and described by Sergeev *et al.* [2003] is shown in Figure 2b. It can be reproduced by our simulations at times

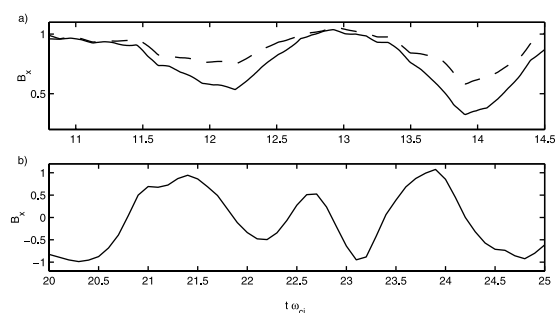


Figure 3. Signatures of current sheet flapping as would be recorded by a virtual spacecraft placed in the environment provided by the simulation and which reproduce the real signature shown in Figure 2. The B_x magnetic field is plotted, normalized to B_0 .

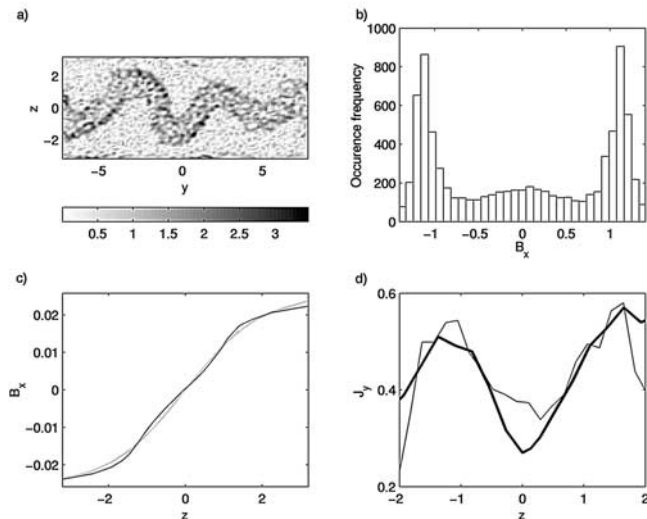


Figure 4. Current density $\sqrt{J_y^2 + J_z^2}$ from the two-dimensional simulation at time $t\omega_{ci} = 20$ (a), B_x (normalized to B_0) occurrence frequency (b), B_x profile as a function of z (solid) and comparison with Harris current sheet (dotted) (the normalization is arbitrary) (c), and current profile from the simulation compared with Geotail observations [Hoshino *et al.*, 2003, Figure 4b] (the original dimensionless units have been scaled to fit the simulation results) (d).

after $t\omega_{ci} = 20$, when the amplitude is sufficient to allow the virtual satellite to cross the current sheet. This is shown in Figure 3b. We note that Cluster observations reveal a flattening of the current sheet in the vicinity of the points where $B_x = 0$, which is associated with current sheet bifurcation. The grid spacing in our three-dimensional simulation is inadequate to resolve this structure.

[13] In agreement with Sergeev *et al.* [2003] and Runov *et al.* [2003], our simulations reveal that the current sheet flapping is mostly in the (y, z) plane, while the tilt in the (x, z) plane is insignificant.

4. Current Sheet Bifurcation

[14] Current sheet bifurcation is revealed both in averages over a number of current sheet crossings, and in single sheet crossings.

[15] The statistical studies of the current sheet presented by Hoshino *et al.* [1996] reveal a bifurcated current profile. An ensemble of neutral sheet crossings is considered and the occurrence frequency of B_x is evaluated. The observed distribution has a peak around the null magnetic region, as also shown by Sergeev *et al.* [2003]. From the distribution of the occurrence of the field B_x , the functional form of the magnetic field as a function of z can be obtained as described by Hoshino *et al.* [1996], and from the gradient of B_x with respect to z it is possible to evaluate the plasma current. The procedure averages over current sheet flapping and the particular motion of the current sheet.

[16] In order to study current bifurcation, we have performed a two-dimensional simulation in the (y, z) plane that allows us to use a more refined grid ($N_y \times N_z = 128 \times 64$). We note that the two-dimensional simulation excludes reconnection. In Figure 4a we show the plot of in-plane current, $\sqrt{J_y^2 + J_z^2}$, at $t\omega_{ci} = 20$. Although there are large

fluctuations, one can detect an increase in the current on the flanks of the current sheet. Following GEOTAIL data analysis, we compute the volume distribution or occurrence frequency of B_x (Figure 4b). The occurrence frequency has peaks at ± 1 due to contributions from the field outside the current sheet, but there is a peak near $B_x = 0$ as in the satellite data [Hoshino *et al.*, 1996, Figure 2; Sergeev *et al.*, 2003, Figure 4]. The function $B_x(z)$ is evaluated as explained by Hoshino *et al.* [1996] (Figure 4c), and is compared with a Harris sheet profile. The current as a function of z (Figure 4d) is depleted at the center and peaked on the flanks of the initial current sheet. (This is unlike the Harris sheet equilibrium, where $\partial B_x / \partial z$ is maximum at $z = 0$, where $B_x = 0$.) The current density profile from GEOTAIL observations is also shown in Figure 4d [Hoshino *et al.*, 1996, Figure 4] and found in remarkable agreement.

[17] Single crossing observations of current sheet bifurcation are shown by Runov *et al.* [2003] and by Sergeev *et al.* [2003]. We focus on Figure 3c by Sergeev *et al.* [2003], which shows reduced $\partial B_x / \partial z$ in the central current sheet (reduced current density) and enhanced gradient at the boundary (enhanced current density). In Figure 5, where we plot a number of B_x profiles as a function of z , at different values of y , the features of the magnetic field structure shown by satellite observations are reproduced by the simulations.

[18] We also remark that our simulation recovers the observations by Geotail on 23 April, 1996, which show that a positive $d|B_x|/dt$ corresponds to an intense current density J_y [Asano *et al.*, 2003], a signature of current sheet bifurcation.

[19] The conclusion of our simulation study, which excludes reconnection, is that current bifurcation is the effect of a current aligned instabilities (i.e., LHDI and KH) and it is not due to the reconnection process.

5. Reconnection

[20] Satellite observations typically reveal reconnection either by detecting inflow and outflow plasma jets, which can be very noisy [e.g., Asano *et al.*, 2003], or by detecting earthward and tailward plasma jets with velocities of the

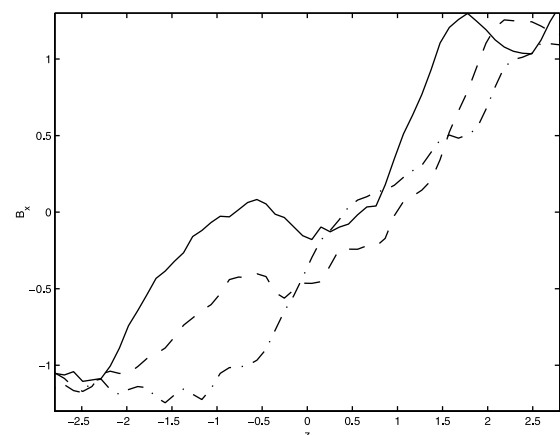


Figure 5. B_x profile as a function of z for different value of y .

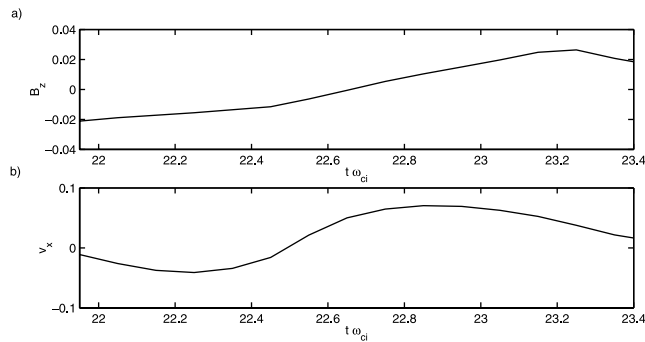


Figure 6. Typical signature of reconnection: during the crossing of the current sheet, the reconnecting field, B_z , changes sign (a) and it is associated to earthward and tailward plasma jets (b).

order of $0.1 V_A$ or bigger [Hoshino *et al.*, 1996], or even by detecting flow reversal [Øieroset *et al.*, 2001].

[21] In fact, in our three-dimensional simulation, not only a kink instability but also a tearing instability develops in the Harris sheet, which leads to the reconnection of the magnetic field lines and outflow and inflow plasma jets. In the present case, the fastest tearing mode grows with $k_x L \approx 0.5$ and mode number $m_x = 2$ in our simulation box, and two magnetic islands grow. Then, the islands merge to form a single island tearing mode that involves the whole domain. The X-line is stationary and aligned to the dawn-to-dusk direction (y direction).

[22] In Figure 6, we display a signature of magnetic reconnection by showing a flow reversal associated with a change in the sign of the reconnecting field. The X-line is passed by the virtual satellite when the system is dominated by a single island. The satellite trajectory crosses the current sheet passing from $z = -0.1 c/\omega_{pi}$ to $z = 0.1 c/\omega_{pi}$ and from $x = -4.5 c/\omega_{pi}$ to $x = -3 c/\omega_{pi}$. The earthward and tailward velocities, detected during the crossing of the current sheet, are of the order of $0.1 V_A$. Satellites also observe subalfvénic flow [Hoshino *et al.*, 1996; Øieroset *et al.*, 2001].

6. Conclusion

[23] We have used the results of three-dimensional and two-dimensional kinetic simulations of Harris current sheet to show that satellite observations of current sheet flapping, current bifurcation, and reconnection can all be explained as a consequence of the instabilities affecting a Harris current sheet. We have chosen to start from a relatively thin and unstable current sheet ($\lambda/d_i = 0.5$) in order to accelerate the plasma dynamics. Such thin current sheets are indeed observed in the magnetotail [e.g., Asano *et al.*, 2003].

[24] We have shown that flapping oscillations can result from a large amplitude KH instability that affects the whole current sheet, for which the scaled frequency and amplitude compare well with satellite observations. The KH instability is due to the velocity shear in the initial conditions and is

independent of the LHDI and tearing instabilities. Both average and single crossing signatures of current sheet bifurcation have been detected in agreement with satellite observations. Current sheet bifurcation appears to be the result of the development of the current aligned instabilities (i.e., LHDI and KH) and is clearly independent of the reconnection. Flow reversal, a signature of reconnection, is also shown in the presence of a changing sign B_z component, due to the growth of the tearing instability.

[25] **Acknowledgments.** The authors gratefully thank M. Hoshino for the permission to use the data plotted in Figure 4 and J. Birn, J. Chen, W. Daughton, I. Furno, M. Taylor, A. Vaivads for helpful discussions. The satellite data has been obtained from Cluster FGM team [Balogh *et al.*, 2001]. This research is supported by the Laboratory Directed Research and Development (LDRD) program at the Los Alamos National Laboratory, by the United States Department of Energy, under Contract No. W-7405-ENG-36 and by NASA, under the “Sun Earth Connection Theory Program”.

References

- Arzner, K., and M. Sholer (2001), Kinetic structure of the post plasmoid plasma sheet during magnetic reconnection, *J. Geophys. Res.*, *106*, 3827.
- Asano, Y., et al. (2003), Evolution of the thin current sheet in a substorm observed by Geotail, *J. Geophys. Res.*, *108*(A5), 1189, doi:10.1029/2002JA009785.
- Balogh, A., et al. (2001), The Cluster magnetic field investigation: Overview of in-flight performance and initial results, *Ann. Geophys.*, *19*, 1207.
- Birn, J., et al. (2001), Geospace Environment Modelling (GEM) magnetic reconnection challenge, *J. Geophys. Res.*, *106*, 3715.
- Brackbill, J. U., and D. W. Forslund (1985), Simulation of low frequency, electromagnetic phenomena in plasmas, in *Multiple Times Scales*, edited by J. U. Brackbill and B. I. Cohen, pp. 271–310, Academic, San Diego, Calif.
- Hoshino, M., et al. (1996), Structure of plasma sheet in magnetotail: Double-peaked electric current sheet, *J. Geophys. Res.*, *101*, 24,775.
- Karimabadi, H., W. Daughton, P. L. Pritchett, and D. Krauss-Varban (2003a), Ion-ion kink instability in the magnetotail: 1. Linear theory, *J. Geophys. Res.*, *108*(A11), 1400, doi:10.1029/2003JA010026.
- Karimabadi, H., P. L. Pritchett, W. Daughton, and D. Krauss-Varban (2003b), Ion-ion kink instability in the magnetotail: 2. Three-dimensional full particle and hybrid simulations and comparison with observations, *J. Geophys. Res.*, *108*(A11), 1401, doi:10.1029/2003JA010109.
- Kokobun, S., et al. (1994), The Geotail magnetic field experiment, *J. Geomagn. Geoelectr.*, *46*, 4.
- Mukai, T. S., et al. (1994), The low energy particle (LEP) experiment on board the Geotail satellite, *J. Geomagn. Geoelectr.*, *46*, 669.
- Øieroset, M., et al. (2001), In situ detection of collisionless reconnection in the Earth’s magnetotail, *Nature*, *412*, 414.
- Runov, A., et al. (2003), Cluster observation of a bifurcated current sheet, *Geophys. Res. Lett.*, *30*(2), 1036, doi:10.1029/2002GL016136.
- Sergeev, V. A., et al. (1993), Structure of the tail plasma/vortex sheet at $\approx 11 R_E$ and its changes in the course of a substorm, *J. Geophys. Res.*, *98*, 17,345.
- Sergeev, V., et al. (2003), Current sheet flapping motion and structure observed by Cluster, *Geophys. Res. Lett.*, *30*(6), 1327, doi:10.1029/2002GL016500.
- Shindler, K., and J. Birn (2002), Models of two-dimensional embedded thin current sheets from Vlasov theory, *J. Geophys. Res.*, *107*(A8), 1193, doi:10.1029/2001JA000304.
- Sitnov, M. I., et al. (2003), A model of the bifurcated current sheet, *Geophys. Res. Lett.*, *30*(13), 1712, doi:10.1029/2003GL017218.
- Zelenyi, L. M., et al. (2002), “Aging” of the Magnetotail thin current sheet, *Geophys. Res. Lett.*, *29*(12), 1608, doi:10.1029/2001GL013789.

J. U. Brackbill and G. Lapenta, Los Alamos National Laboratory, Los Alamos, NM 85744, USA. (lapenta@lanl.gov)

P. Ricci, Dipartimento di Energetica, Politecnico di Torino, Corso Duca degli Abruzzi 24-10129 Torino, Italy. (paolo.ricci@polito.it)